

CFD Analysis and Model Comparisons of Circulating Temperature During Cementing Job

Yanfang Wang, Louisiana State University; Hu Dai, Pegasus Vertex, Inc.

Copyright 2019, AADE

This paper was prepared for presentation at the 2019 AADE National Technical Conference and Exhibition held at the Hilton Denver City Center, Denver, Colorado, April 9-10, 2019. This conference is sponsored by the American Association of Drilling Engineers. The information presented in this paper does not reflect any position, claim or endorsement made or implied by the American Association of Drilling Engineers, their officers or members. Questions concerning the content of this paper should be directed to the individual(s) listed as author(s) of this work.

Abstract

With the development of deep water wells and geothermal wells, it is still a challenge to accurately predict heat transfer in wellbore modeling. Bottom Hole Circulating Temperature (BHCT) is a significant parameter for cement design, which may cause cement displacement problem or failure due to inappropriate temperature evaluation and prediction. Even though computer simulators and correlations had been developed to match with field measurement data, it is still unconvincing or too sophisticated for field utilization. In this study, a simplified simulator was presented to dynamically calculate wellbore temperatures. For verification, a state-of-the-art large scale Computational Fluid Dynamics (CFD) wellbore model had been developed and numerical simulations had been conducted to investigate heat transfer during cementing process. Multiple phases were involved including mud, spacer, cement and displacement fluid, whose rheological models were all treated as Yield Power Law (YPL) with different physical and thermal properties. The simulation results included the BHCT evolution with time and wellbore temperatures at end of cementing job. The proposed simulator was verified by providing comparison of simulation results from the developed simulator and CFD solver. Because of the large scale of this CFD model, it was able to realize the near wellbore formation cool-down effect at the end of the cementing job.

An offshore field case with multiple geothermal gradients was used to validate the proposed simulator. At the end, with the proposed simulator, sensitivity analysis of BHCT with the influences of pump rate and number of injected bottom-ups for pre-job operation was also presented to improve the understanding of heat transfer in wellbore and near wellbore region, also to identify practical guidelines and solutions to optimize cementing design.

This study presented here not only serves to verify and validate the proposed simulator used for engineering purpose, but also illustrated what the capabilities of the new CFD model are, and what could be achieved in the very near-future in better simulating and thereby planning for complex cementing scenarios such as offshore wells and geothermal wells.

Introduction

It has long been known that temperature during circulation and after cement placement is one of the most important parameters for the design of a slurry and the success of cement

jobs. BHCT is influenced by the following parameters: circulation time, circulating rate, fluid inlet temperature, geothermal temperature (including the sea), wellbore geometry including (pipe, hole dimensions, well deviation, presence of riser), sea depth and currents, fluid densities and thermal properties. The normally used American Petroleum Institute (API) correlations had been realized that it did not consider important parameters affecting the temperature evolution, especially in offshore well operations (Wedelich et al., 1987, Guillot et al, 1993). The reason is that API correlation used the True Vertical Depth (TVD) and a single temperature gradient (computed from the Bottomhole Static Temperature (BHST)) to make the estimations. However, it didn't include factors such as circulation rate and time, temperature of the injected fluid and sea temperature and currents. Computer thermal simulators had been developed to fill this gap. However, the validation of simulator models is difficult or unconvincing, as there always exists a set of input parameters that can match observed temperature on a particular well but not all other wells.

Goodman et al. (1988) developed improved circulating temperature correlations for various cementing scenarios. The correlations were developed from wellbore thermal simulators' results and compared to field measurements. Guillot et al. (1993) proposed a numerical simulator for calculating cementing temperature, which had been created and used in a cementing software. This model selected API database wells to allow a proper validation. A minimal data set consists of the description of well geometry, flow rate, inlet temperature, type of fluid pumped, BHST, fluid density, fluid rheology and time at which the measurements were performed. However, there was no information concerning formation type, well deviation or the presence of multi-geothermal gradients was available. So, in their study, formation type was assumed to be sand for all cases, and wells were assumed vertical, and a linear geothermal gradient. The outcome included wellbore fluid temperature, and surrounding formation temperature as function of depth and time. As result, sensitivity of formation type to temperature prediction was small. In Calvert and Griffin's (1998) study, two simulators were used to compare circulating temperature with API prediction. The results of simulation with drill pipe in hole showed the inaccuracy of using API schedules in deep water. The simulators were also used to calculate circulating temperature when circulating with casing in the hole.

Nowadays, the application of CFD tool for simulation had been widely used from mechanical, chemical to petroleum industries. CFD modeling technique has been used in recent years to unravel the dynamic behavior of fluid movements with reference to cementing (Chen et al., 2014; Xie et al., 2015; Karbasforoushan et al., 2016; Durmaz et al., 2016; Enayatpour and Eric van Oort, 2017). Heat transfer problem in wellbore modeling also involves fluid flow dynamics behavior and plays a significant role in the planning of cementing design. However, there is very limited literature associated with prediction of wellbore temperature for cementing operations using CFD simulation tools. Tarom and Hossain's (2012) study proposed a practical method through development of a simplified semi-analytical model to apply for predicting temperature profile along the wellbore. For verification of their proposed model, their study carried out numerical simulations through ANSYS Fluent to simulate heat transfer in wellbore with multiple layers. The simulated case was a transient case of 2-D wellbore which surrounded by different layers of tubing, casing, cement sheaths and formation. This study threw light on the capabilities of CFD package, e.g. Fluent, to simulate wellbore fluid flow and heat transfer between wellbore fluid and its surroundings.

In this study, a simplified dynamic temperature modeling technique was proposed and has now been embedded in cementing software, CEMPRO, for oilfield applications. For validation, a 2-D wellbore model with the whole wellbore cross section was developed and simulated using ANSYS Fluent flow modeling software. Some simulation results including BHCT with time, and wellbore temperatures (temperature inside casing, annulus temperature between casing and formation) at the end of cementing job. Sensitivity analysis was also carried out by the proposed model to reveal the evolution of BHCT with time, provide guidelines for circulation operations or cementing design purposes.

Wellbore Thermal Simulator Description

The proposed simulator was fulfilled by solving a series of energy equations including inside casing, on casing wall, on inner string wall, in stationary annulus, interface of wellbore and formation and formation itself. In stationary fluid, walls, cased hole sections and formations, conductive heat transfer in radial direction was occurred. And convective heat transfer was occurred in inner string/pipe, annulus and outside pipe or riser above mudline. Gauss-Seidel iterative method was used to solve these equations.

The energy equation inside annulus in forward operation with two different fluids was expressed as Eqn (1):

$$\frac{[(\rho_1 V_1 C_1 + \rho_2 V_2 C_2) T_{a,j}]^{N+1} - [(\rho_1 V_1 C_1 + \rho_2 V_2 C_2) T_{a,j}]^N}{\Delta t} = 2\pi r_{ID} (U_{ID} h_1 + U_{ID} h_2) (T_{a-1,j}^{N+1} - T_{a,j}^{N+1}) - 2\pi r_{OD} (U_{OD} h_1 + U_{OD} h_2) (T_{a,j}^{N+1} - T_{a+1,j-1}^{N+1}) + \rho_2 q_2 C_2 T_{a,j+1}^{N+1} - \rho_1 q_1 C_1 T_{a,j}^{N+1} \quad (1)$$

For the energy equation inside drill pipe in forward operation, Eqn (2) gave:

$$\frac{[(\rho_1 V_1 C_1 + \rho_2 V_2 C_2) T_{a,j}]^{N+1} - [(\rho_1 V_1 C_1 + \rho_2 V_2 C_2) T_{a,j}]^N}{\Delta t} = 2\pi r_{OD} (U_{OD} h_1 + U_{OD} h_2) (T_{a+1,j}^{N+1} - T_{a,j}^{N+1}) + (\rho_1 q_1 C_1 -$$

$$\rho_2 q_2 C_2) (T_{a,j-1}^{N+1} - T_{a,j}^{N+1} - T_{a,j}^N) \quad (2)$$

where C_1 and C_2 are the heat capacities of fluid 1 and fluid 2, V_1 and V_2 are fluid velocities, ρ_1 and ρ_2 are fluid densities. U_{OD} and U_{ID} are overall heat transfer coefficients at fluid-formation interface and drill pipe - annulus interface respectively. The terms q_1 and q_2 are volumetric flow rates, and h_1 and h_2 are convective heat transfer coefficients of fluid 1 and fluid 2.

For the meshing, additional grid points are set for wellbore configuration, and pipe section change. The mesh in radial direction first sets grid points to calculate temperature inside pipe, on the pipe wall, inside annulus and wellbore/rock interface. Mesh extends into formation with an increasing mesh size from the well/rock interface. Examples of schematics of discretization for onshore and offshore wells (with risers) were shown in Fig. 1 and Fig. 2, respectively.

For cased holes, the thermal resistance and overall heat transfer coefficient between annulus and wellbore/formation interface were given by Eqn (3) and Eqn (4):

$$R_{casing\ layers} = \sum_{i=1}^N \left(\frac{\ln(r_{OD}/r_{ID})}{2\pi L k_{steel}} + \frac{\ln(r_{Bit}/r_{OD})}{2\pi L k_{fluid/cement}} \right) \quad (3)$$

$$U = \frac{1}{\frac{1}{2\pi L r_a h_a} + \sum_{i=1}^N \left(\frac{\ln(r_{OD}/r_{ID})}{2\pi L k_{steel}} + \frac{\ln(r_{Bit}/r_{OD})}{2\pi L k_{fluid/cement}} \right)} \quad (4)$$

For offshore well with water depths and installation of risers, the thermal resistances were given by Eqn (5) and Eqn (6) for annulus of water and annulus of air, respectively:

$$R_{Annulus-water} = \frac{1}{2\pi L} \left(\frac{1}{h_a r_{ID}} + \frac{\ln(r_{OD}/r_{ID})}{k_{steel}} + \frac{1}{h_{water} r_{OD}} \right) \quad (5)$$

$$R_{Annulus-air} = \frac{1}{2\pi L} \left(\frac{1}{h_a r_{ID}} + \frac{\ln(r_{OD}/r_{ID})}{k_{steel}} + \frac{1}{h_{air} r_{OD}} \right) \quad (6)$$

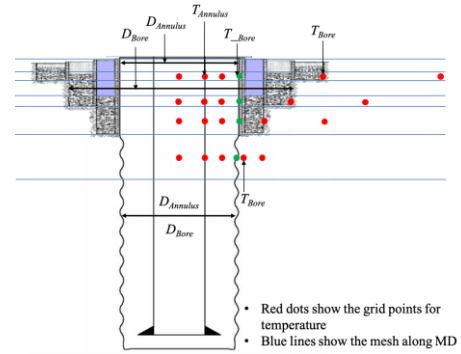


Fig. 1 Discretization of onshore well with stationary annulus

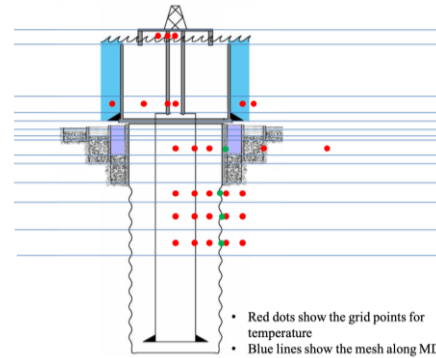


Fig. 2 Discretization of offshore well with riser

Numerical Simulations for Verification

ANSYS Fluent numerical simulator is a package that has broad capabilities to model multiphase flow, turbulence, heat transfer, etc. for a wide range of industrial applications including drilling, cementing, cutting transportation. Fluent has been used as a tool to validate and simulate cementing process to calculate Displacement Efficiency (DE), using Volume of Fluid (VOF) model to capture volume fraction of each phase in the fluid domain (Wang and Dai, 2018). Fluent also can solve the heat transfer problems using energy equations. Depending on the problem we are solving, natural, forced and mixed heat convection mechanism, conjugate (fluid/solid) heat transfer, radiation heat transfer mechanism, transient and steady-state heat transfer conditions are some of the capabilities embedded in Fluent software. Therefore, the ANSYS Fluent can be a powerful and reliable tool to solve heat transfer problems in cementing process. The ANSYS Fluent was chosen to compare with our thermal model for verification.

The energy equation is expressed in the following form (Fluent theory Guide, 2010):

$$\frac{\partial}{\partial t}(\rho E) + \nabla \cdot (\vec{v}(\rho E + p)) = \nabla \cdot (k_{eff} \nabla T - \sum_j h_j \vec{J}_j + (\vec{\tau}_{eff} \cdot \vec{v})) + S_h \quad (7)$$

Where k_{eff} is the effective conductivity, and \vec{J}_j is the diffusion flux of species j . The first three terms on the right-hand side of Eqn (7) represent energy transfer due to conduction, species diffusion, and viscous dissipation, respectively. S_h includes the heat of chemical reaction, and any other volumetric heat sources.

In this study, a large scale 2-D wellbore model was created. In this model, it is supposed that there are fluids into wellbore and annulus section and the solids parts include casing and formation. Therefore, the solution is for the mixing of fluid and solid including different properties for each material.

Geometry

Among various options of casing and borehole sizes, we chose a very frequently used wellbore size for simulation. The hole I.D. is 12 1/4 inches, and the casing O.D. is 9 5/8 inches, casing I.D. is 8.921 inches. The well is supposed to be a vertical onshore well with measured depth of 1200 ft. There is 0.2 ft gap between casing bottom and hole bottom to simulate what happens in an actual wellbore. Modeling deeper wells is not feasible due to very long computation time and limitations of the program. A simplified display for the model geometry was shown in Fig. 3.

The main purpose of this simulation is to calculate the BHCT during cementing job, and wellbore temperature at the end of job. To obtain the results more rapidly, this large and long model was meshed to keep the node number at a minimum while maintaining a good degree of accuracy. Achieving this degree required considerable amount of experimenting and time. Quadrilateral elements with four nodes, which has fluid velocity, pressure, temperature was used for meshing. To achieve structured mesh, multi-zone Quad/Tri method was applied in meshing method option. Since temperature change on both vertical direction and radial direction were considerably

slow, the mesh size of the formation was selected to be 4.4 ft x 6.2 ft. For the wellbore, the vertical mesh size is 1.5 ft, and horizontally all the conduits and casing were meshed to have at least 3 nodes. At the wellbore bottom, there is relatively large fluid gradient happened, so that region is specially taken into account and has denser elements to reduce calculation errors. A close-view of the meshing results at bottom hole can be seen in Fig. 4. Overall, this 2-D wellbore and formation model had 45817 nodes, and 12333 elements in total.

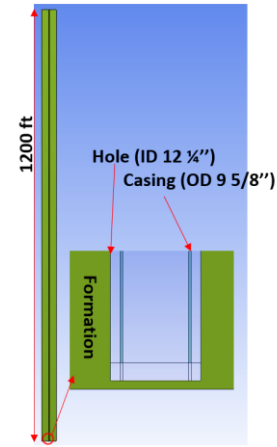


Fig. 3 A display of the 2-D cross section formation and wellbore model

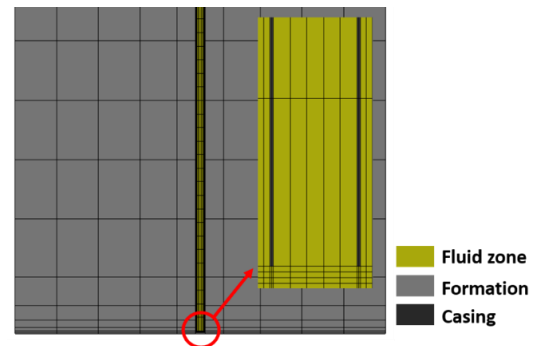


Fig. 4 A close-view of meshing information at formation and bottom hole

Physical Settings for Simulation Work

After meshing the geometry, the model was required to define specified conditions for computations. Throughout the whole simulation, there are four different kinds of fluid materials and two solid materials to be defined. Lists of thermal and physical properties for fluids and solids as input data were shown in Table 1 and Table 2, respectively.

Initially, the fluid domain was occupied by native mud (primary phase), and then spacer, cement and displacement fluid were pumped into wellbore in sequences, which were all considered as secondary phases. All fluids were assumed to be incompressible and there was no phase change in the workstring, annulus and formation. For simplicity, the injection rate for each phase was kept constant during the simulation. The inlet temperature was assumed to be the same, 75 °F. The

formation temperature was simply supposed to have single temperature gradient of 1.5 °F/100 ft. The surface temperature was 75 °F. There was no source or sink of heat in wellbore and formation. Specially, cement hydration heat is not included. A list of pumping schedule was shown in Table 3. The injected amount of spacer is 60 bbl. Cement fluid was then injected following spacer, the injected volume is one annulus volume. Then, the last fluid, displacement fluid was injected to push cement in place. The injected volume of displacement fluid is equal to the inside casing volume.

Table 1. Input data of fluid properties for cementing simulation

Fluid List	Density (kg/m ³)	Rheology	Thermal Conductivity (w/m-c)	Specific Heat, C _p (j/kg-c)	Injection Rate (bpm)
Mud	1800	YPL k = 0.6 n = 0.54	1.385	3768	0
Spacer	1800	YPL k = 0.6 n = 0.54	1.385	2512	8
Cement	1850	YPL k = 0.55 n = 0.57	1.385	3920	8
Disp. fluid	1800	YPL k = 0.6 n = 0.54	1.385	3768	8

Table 2. Input data of solid properties for cementing simulation

Solid List	Density (kg/m ³)	Thermal Conductivity (w/m-c)	Specific Heat, C _p (j/kg-c)
Casing	7848.8	45	879.2
Formation	2240.8	1.59	1256

Table 3. A list of pumping schedule used for model simulations

Pumping fluid	Volume (bbl)	Time (min)	Elapsed time (min)
Spacer	60	7.5	7.5
Cement	66.944	8.368	15.868
Disp. fluid	92.781	11.598	27.466

The initial temperature of the wellbore was the same as geothermal temperature. The temperature was constant at the same depth. In formation, there was only heat conduction and no convection (fluid flow) in formation included in this study. For boundary conditions, we set inlet at surface as velocity inlet condition, and outlet as mass flow-out condition. The mass flow rate for each phase was specified. The heat transfer between solid and fluid at the interfaces between casing and annulus fluid, interfaces between fluid and formation was achieved by

matching these interfaces at different zones into coupled walls. It is a crucial step in conjugate (solid/fluid) heat transfer modeling process because it enabled to compute conduction of heat through solids (casing or formation) and coupled with convective heat transfer in fluid. The very far-away formation border, or formation wall had not been disturbed and kept the geothermal temperature. However, the near-wellbore region of formation should have temperature variance.

Simulation Results

After setting the initial and boundary conditions, the numerical solver was needed to be set to simulate a reasonable cementing job, which requires a step-by-step solution process during simulation. In this specific study, different fluids were injected and the inlet condition was changed following the procedures. Throughout the whole simulation, the VOF fluid flow model and energy equation were used, and laminar flow model was also used because these fluids were flowing in laminar flow pattern. Fig. 5 gave an example of velocity contour based on the Y-axis direction, located at bottom hole section. To view actual fluid flow downward through the casing and flow upward at the casing shoe to annulus, a velocity vector was also plotted in Fig. 5. We can see at bottom hole, there was large fluid velocity gradient in which the fluid velocity suddenly changes to smaller value close to 0. Therefore, we need denser meshes at the bottom hole region, also, we can see that there was no velocity at the walls.

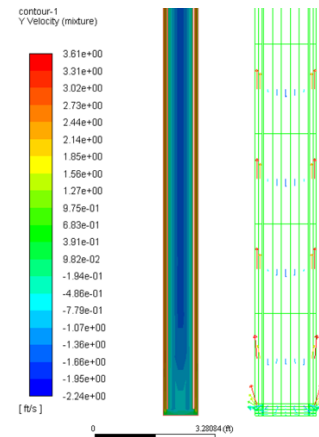


Fig. 5 Mixture velocity contour and velocity vector at Y-axis direction near bottom hole

Initially, the highest temperature occurred at the bottom hole, which was 93 °F by calculating from a linear geothermal gradient of 1.5 °F/100 ft and surface temperature of 75 °F. However, during cement placement operation, the hottest temperature will occur at some depth above the bottom hole in the annulus. During the circulation, the surface fluid is pumped into wellbore and heated up in the path traveling down to the bottom by gaining heat from annulus fluid. After the fluid reaches the bottom hole it turns into the annulus and flows up through the annulus. The annulus fluid will gain heat from formation and also lose heat to the workstring fluid at the same

time. In the near bottom hole section, the annulus fluid will gain more heat than it loses, resulting in being heated up and temperature increases. At a certain depth, the heat gained and heat lost by the annulus fluid reach a balance and the fluid temperature reaches its maximum. The heat gained by the annulus fluids was then less than the heat they lost, which caused a decrease of temperature when flowing above that certain depth. The maximal temperature is initially at bottom hole and will move up during circulation. The depth where the maximal temperature occurs at the end of job depends on fluid properties, hole size, pump rate and circulation time.

Fig. 6 was a plot to compare the calculated BHCT. As mentioned previously, there are four types of fluids involved in cementing job, e.g. mud, spacer, cement, displacement fluid. Initially, the fluid domain was occupied by mud, then spacer was injected at inlet to displace mud in the wellbore and flow till bottom hole, then circulated up to annulus. At the initial 6 minutes, the BHCT had a good match between the simulator and Fluent, then the discrepancy started to occur. The largest difference was occurred around 10 minutes from the start of injection, which was approximately 2 °F, which was fairly acceptable considering this large scale geometry and some acknowledged errors such as computer round-off errors. The discrepancy tended to decrease with time and showed a good match again in the displacement fluid injection stage, with an error of less than 1 °F. The intermixing behavior between multiple phases makes it difficult to simulate the actual fluid velocities and viscosities since these fluids are all non-Newtonian fluids and have complex rheological properties. What's more, the wall roughness condition added more challenges to predict the actual position of the injected fluid and their movement at downhole condition. However, as the circulation continues, the bottom hole temperature will stabilize and remain at constant temperature as predicted in both simulators.

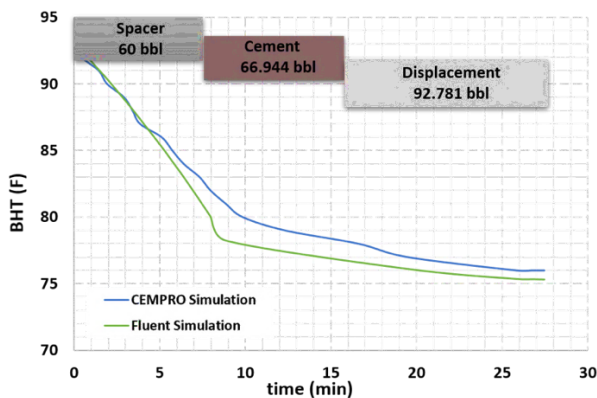


Fig. 6 Comparison results of BHCT between the proposed simulator and Fluent solver

At the end of cementing simulation, it is also important to view the temperature profile through the entire wellbore, basically inside the conduit and annulus. Table 4 and Table 5 showed the comparison results of the performances of the

proposed simulator (CEMPRO) and CFD solver, showing the temperature at inside casing and temperature at annulus at 10 different depths. In Table 4, by comparisons of inside casing temperature, we can see the percentage error between 0 and 1.2%. In Table 5, compared with Table 4, the percentage errors of annulus temperatures were bigger than those of inside casing temperatures. But the errors were ranged from 0.9% to 3.2%, which clearly demonstrated the proposed simulator had good agreement with the Fluent solver.

Table 4. Inside casing temperature comparisons at different depths

MD (ft)	Inside Casing. T (°F) (Fluent)	Inside Casing. T (°F) (CEMPRO)	Percentage error (%)
0	75	75	0
122	75	75	0
305	75.1	75	0.1
488	75.1	76	1.2
549	75.2	76	1.1
671	75.2	76	1.1
854	75.2	76	1.1
1000	75.2	76	1.1
1098	75.3	76	0.9
1200	75.3	76	0.9

Table 5. Annulus temperature comparisons at different depths

MD (ft)	Ann. T (°F) (Fluent)	Ann. T (°F) (CEMPRO)	Percentage error (%)
0	76.7	78	1.7
122	76.3	78	2.2
305	75.9	78	2.8
488	75.7	78	3
549	75.6	78	3.2
671	75.6	77	1.9
854	75.4	77	2.1
1000	75.4	77	2.1
1098	75.3	77	2.3
1200	75.3	76	0.9

In Fig. 7 we showed comparison results of formation temperature contour plot to demonstrate the formation cool-down effect near wellbore at the end of cementing job. To clearly see what happened in near wellbore region, a partially zoomed image can see the differences between the initial and end times. Initially, the temperature near wellbore were the same with far-away formation temperature. A zoomed view in a partial region shows no temperature change near wellbore region. At the end of job, from the zoomed view image we can see the blue line represented the wellbore temperature was close to 75°F. The formation near wellbore was cooled down with the evidence of concavity near the wellbore. However, it is

necessary to state that this is only the results after 27 mins, we can see more obvious change when the simulation time increases.

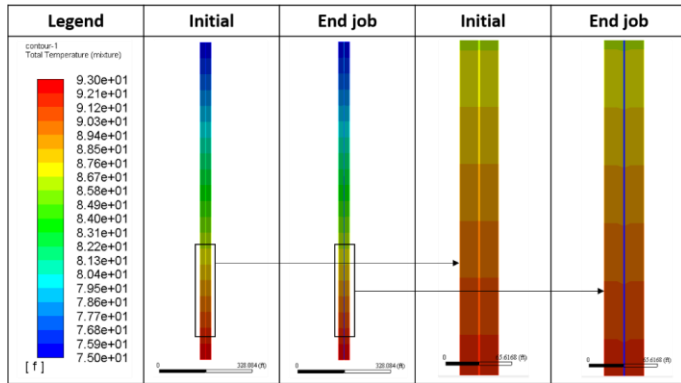


Fig. 7 Formation temperature distributions at initial and end of job

Comparison Results with Field Data

The field case we chose was from an offshore well (Chen and Novotny, 2003). This well was a deep water well with multiple geothermal gradients. The total depth is 5778 ft with water depth of 3780 ft. The circulation fluid returned to surface with a riser O.D. of 21 inches and riser I.D. of 19 3/4 inches, as shown in Fig. 8. The casing size was 20 inches. The circulation fluid, basically seawater, was pumped into wellbore through a 5 inches drill pipe to the circulation depth of 5721 ft, and then fluid returned to surface through annulus. In order to measure the wellbore temperature change, three gauges were installed: one at bottom hole depth, 5721 ft to measure BHCT, the other two installed at annulus, depths at 0 ft and 4786 ft, to record the return fluid temperature and annulus temperature, respectively. Fig. 8 also plotted the static temperature profile before circulation. The ambient temperature was 77 °F and Bottom Hole Static Temperature (BHST) was 59 °F.

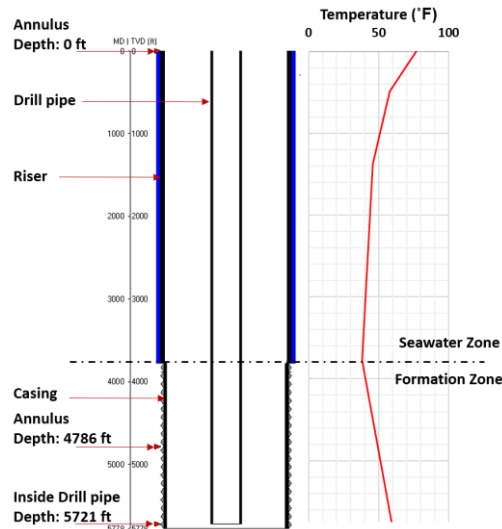


Fig. 8 Offshore well configuration and static temperature profile before circulation

The temperature comparisons between the proposed simulator and field measured data were investigated. The temperatures at three different depths where the gauges were installed were listed in Table 6, Table 7 and Table 8, respectively. The times that were measured were 20 mins, 40 mins and 60mins (end of job). The differences were calculated as well. Fig. 9 plotted measured and simulated temperature at three sensor depths. The BHCT dropped rapidly during the first 5 mins circulation. Compared the results at three locations, the percentage errors were ranged from 1% up to 11.5%. Taken into account the insufficient information about the cementing operations, the simulation provided a generally acceptable result.

Table 6. Measured and simulated temperatures at circulation depth (5721 ft)

time (min)	Measured (°F)	Simulated (°F)	Percentage error (%)
20	51.5	54	4.9
40	53.3	57	6.9
60	54.4	58	6.6

Table 7. Measured and simulated temperatures at depth 4786 ft

Time (min)	Measured (°F)	Simulated (°F)	Percentage error (%)
20	51.5	52	1
40	53.3	55	3.2
60	53.9	57	5.8

Table 8. Measured and simulated temperatures at return surface

time (min)	Measured (°F)	Simulated (°F)	Percentage error (%)
20	68.9	61	11.5
40	65.7	61	7.2
60	64.8	62	4.3

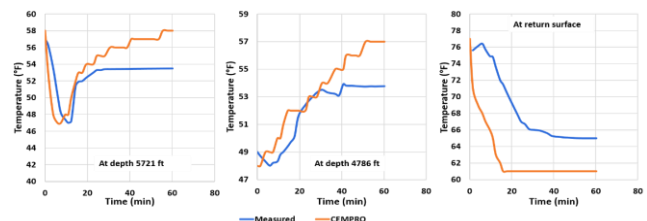


Fig. 9 Measured and simulated temperatures at circulation depth of 5721 ft, at depth of 4786 ft, and at return surface

Effects of Pre-cementing Job on Wellbore Temperature

After verified with CFD solver and validated with field

measured data, a series of sensitivity analysis were carried out to investigate the effects of variables, including pump rate, circulation time which is determined by the number of injected bottom-ups. Before pumping cement, a designated fluid, usually mud, is required to be pumped into wellbore and circulated up one or more bottom-ups to cool down the wellbore temperature. To investigate heat transfer with one single fluid circulation through wellbore, a typical well configuration and several case scenarios were generated for the sensitivity analysis. The well was an onshore vertical well with measured depth of 10,000 ft. Hole I.D. is 12 ¼ inches, casing O.D. is 9 5/8 inches, and I.D. is 8.921 inches. The circulating fluid was drilling mud with density of 11.5 ppg, the rheological model is Herschel-Bulkley model where K is 1.253 lbf-sⁿ/100ft², n is 0.54. The yield point is 2.5 lbf/100ft², and the gel strength is 2.5 lbf/100ft². The formation has a single linear geothermal gradient of 1.5 °F/100 ft. Ambient temperature is 75 °F.

Fig. 10 plotted the annulus profiles after one bottom-up circulation with pump rates of 5 bpm, 15 bpm and 25 bpm. Initially, the annulus temperature was the same as geothermal temperature from 75 °F at surface to 450 °F at bottom hole. After circulation, at certain depth the annulus temperature above that depth increased and annulus temperature decreased below that depth. And as we expected, initially the highest temperature was occurred at bottom hole, but the highest temperature was occurred at upper annulus depth above the bottom hole at the end of circulation. With flow rate of 5 bpm, the depth of hottest temperature was around 8000 ft. With the increase of flow rate from 5 bpm to 15 bpm, the depth of hottest temperature increased to 8500 ft. And with the flow rate of 25 bpm, the hottest temperature was occurred at 8800 ft.

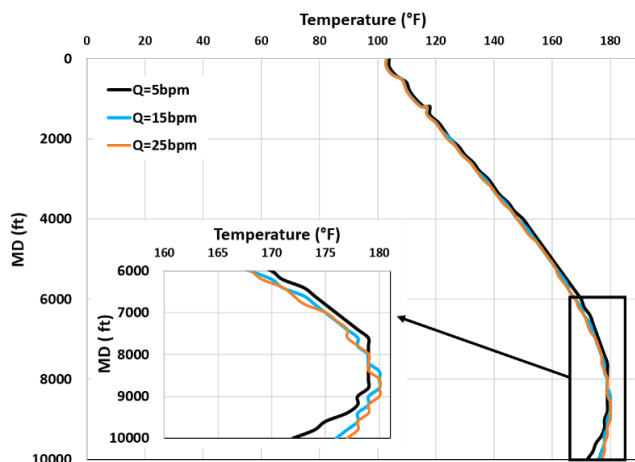


Fig. 10 Annulus temperature profile after one bottom-up circulation at various pump rates

The BHCT is the ultimate result of heat transfer between circulation fluid and formation. Fluid viscosity, fluid thermal property, pump rate, circulation time, and hole size all have impact on BHCT and should not be ignored. Fig. 11 plotted the BHCT with the increased number of injected bottom-up circulations. The flow rates considered for analysis were 5 bpm,

10 bpm, 15 bpm and 20 bpm. Circulation time was also plotted with BHCT because with different flow rates, the circulation times were also different even with the same number of bottom-ups. First, with the increased number of bottom-ups, the circulation times were increased for each scenario with different flow rate. Second, with the increased number of bottom-ups, the BHCT was reduced up to 20 °F from 1 bottom-up to 2 bottom-ups, and was reduced 10 °F from 2 bottom-ups to 3 bottom-ups. Compared between these different pump rates, the BHCT was the lowest with pump rate of 5 bpm at and before 3 bottom-up circulations. With circulation of 4 bottom-ups, the BHCT was the same even with different flow rates. However, the 5 bpm scenario would result in the longest circulation time, which was not a good choice. This plot can guide us to demonstrate that when several bottom-ups circulations are required, it is necessary to pump with high flow rates to reduce the circulation time and achieve an equivalent result to pumping with low flow rates. On the other hand, BHCT decreases with the increase number of bottom-up circulations, but with a reduced decreasing rate. It is recommended that less than 5 bottom-ups circulations would achieve a good wellbore conditioning result.

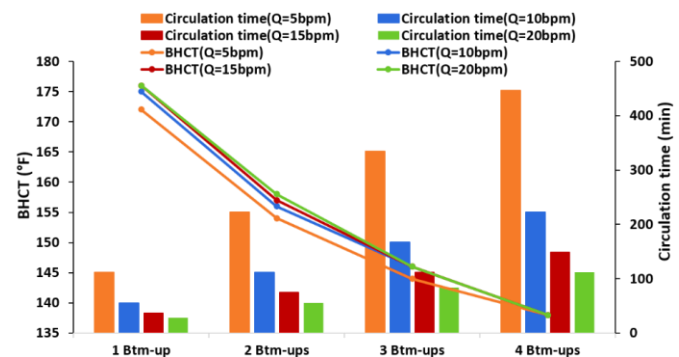


Fig. 11 Effect of number of injected bottom-up circulations on BHCT at various pump rates

Conclusions

In this study, the proposed simulator that had been used in cementing software, CEMPRO, were compared with CFD Fluent solver. Numerical simulations done by CFD flow modeling technique was used to verify the proposed simulator. To mimic the actual cementing operation, pumping different fluids in sequences were fulfilled to unravel dynamic wellbore temperature and formation temperature variance. The purpose of this study is not only to validate the reliability of the proposed thermal simulator, also to justify how effectively the proposed simulator can be used to solve similar thermal problems by saving long computational time which is not desirable by the industry for a routine engineering calculation. In general, based on the CFD verification, offshore field case validation and sensitivity analysis performed in this study, the following conclusions were made:

1. The wellbore thermal simulator technique and methodology are appropriate and provide acceptable simulation results if given enough job details.

2. From the CFD simulation and the proposed simulator comparison, we observed that BHCT rapidly decreases during the spacer fluid injection, and gradually remain lightly decrease or steady at end of job.
3. Sensitivity analysis with various pump rates demonstrated that the impact of pump rate to BHCT and the depth of hottest temperature increased with the pumping rate.
4. As expected, BHCT continues to decrease with the increase number of bottom-up circulations, but with a reduced decreasing rate. As more bottom-ups circulations are required, higher pumping rates are recommended to reduce the circulation time. Economically, it is recommended that the pumped volume should be less than 5 bottom-ups circulations.

Acknowledgments

The authors would like to express the appreciation to the management of Pegasus Vertex, Inc. for permission to publish this paper.

Nomenclature

<i>CFD</i>	= <i>Computational Fluid Dynamics</i>
<i>BHCT</i>	= <i>Bottomhole Circulating Temperature, °F</i>
<i>API</i>	= <i>American Petroleum Institute</i>
<i>TVD</i>	= <i>True Vertical Depth, ft</i>
<i>BHST</i>	= <i>Bottomhole Static Temperature, °F</i>
<i>MD</i>	= <i>Measured Depth, ft</i>
<i>DE</i>	= <i>Displacement Efficiency</i>
<i>VOF</i>	= <i>Volume of Fluid</i>
<i>YPL</i>	= <i>Yield Power Law</i>

References

1. Fluent Theory Guide, version 13.0, ANSYS Inc., 2010, USA.
2. Zhongming Chen and Rudolf J. Novotny: "Accurate Prediction Wellbore Transient Temperature Profile Under Multiple Temperature Gradients: Finite Difference Approach and Case History." SPE 84583. SPE Annual Technical Conference and Exhibition, Denver, Colorado, October, 5-8, 2003.
3. D. G. Calvert and T. J. Griffin, Jr.: "Determination of Temperatures for Cementing in Wells Drilled in Deep Water." IADC/SPE 39315. The 1998 IADC/SPE Drilling Conference, Dallas, March, 3-6, 1998.
4. H. Wedelich, M. A. Goodman and J. W. Galate: "Key Factors That Affect Cementing Temperatures." SPE/IADC 16133. The 1987 SPE/IADC Drilling Conference, New Orleans, March 15-18, 1987.
5. M.A. Goodman, R. F. Mitchell, H. Wedelich, J.W. Galate, and D.M. Presson: "Improved Circulating Temperature Correlations for Cementing." SPE 18029. The 63rd Annual Technical Conference and Exhibition of the Society of Petroleum Engineers, Houston, October, 2-5, 1988.
6. Frederic Guillot, J.M. Boissault and J.C. Hujeux: "A Cementing Temperature Simulator To Improve Field Practice." SPE/IADC 25696. SPE/IADC Drilling Conference, Amsterdam, February, 23-25, 1993.
7. Chen Z., Chaudhary S. and Shine J.: "Intermixing of Cementing Fluids: Understanding Mud Displacement and Cement Placement." IADC/SPE 167922. IADC/SPE Drilling Conference and Exhibition, Fort Worth, Texas, 4-6 March, 2014.
8. Karbasforoushan H., Ozbayoglu, E.M., Miska, S. Z., Yu M., and Takach N.: "On the Instability of Cement-Fluid Interface and Fluid Mixing." SPE-180322-MS. SPE Deepwater Drilling & Completions Conference, Galveston, Texas, September, 14-15, 2016.
9. Xie L., Chaudhary, S., and Chen Z.: "Analysis of the Effect of Eccentricity on Displacement of Non-Newtonian Fluid with a Hybrid Method." SPE-174909-MS. SPE Annual Technical Conference and Exhibition, Houston, Texas, September, 28-30, 2015.
10. Durmaz S., Karbasforoushan H., Ozbayoglu, E.M., Miska, S. Z., Yu M., Takach N., and Aranha P.E.: "Mixing of Cement Slurries During Cement Plug Setting." SPE-180338-MS. SPE Deepwater Drilling & Completions Conference, Galveston, Texas, September, 14-15, 2016.
11. Enayatpour S. and Eric V.O.: "Advanced Modeling of Cementing Displacement Complexities." SPE-184702-MS. SPE/IADC Drilling Conference, The Hague, The Netherlands, March 14-16, 2017.
12. N. Tarom and M.M. Hossain: "Using ANSYS to Realize a Semi-Analytical Method for Predicting Temperature Profile in Injection/Production Well." International Scholarly and Scientific Research & Innovation v. 6, No.12, 2012.
13. Wang, Yanfang and Hu Dai: "Parametric Analysis of Efficiency Using an Efficient Mud Displacement Modeling Technique." AADE-18-FTCE-096, AADE Fluids Technical Conference and Exhibition, Houston, April 10-11, 2018.